

## Electronic Supplementary Information

### **Transparent, mechanically robust, and ultrastable ionogels enabled by hydrogen bonding between elastomers and ionic liquids**

Ziquan Cao,<sup>a</sup> Hongliang Liu\*<sup>b</sup> and Lei Jiang<sup>ab</sup>

*<sup>a</sup> Key Laboratory of Bio-Inspired Smart Interfacial Science and Technology of Ministry of Education, School of Chemistry, Beihang University, Beijing 100191, P. R. China*

*<sup>b</sup> CAS Key Laboratory of Bio-inspired Materials and Interfacial Science, Technical Institute of Physics and Chemistry, Chinese Academy of Sciences, Beijing 100190, P. R. China*

Corresponding author's email address: [liuhl@mail.ipc.ac.cn](mailto:liuhl@mail.ipc.ac.cn)

## Experimental Section

**Materials:** Unless otherwise specified, all starting materials were purchased from J&K Chemical Ltd., China. Ethyl acrylate (EA, 99%) was filtrated through a column of basic alumina to remove the inhibitor. Ethylene glycol dimethacrylate (EGDMA, 98%) and phenylbis (2, 4, 6-trimethylbenzoyl) phosphine oxide (PBPO, 97%, a white light photoinitiator) were used without further purification. A series of ionic liquids with different cation and anion structures (as shown in Fig. S3), *i.e.*, N-hexyl pyridinium bis(trifluoromethyl sulfonyl)imide ([HPy][NTf<sub>2</sub>]), N-butyl-N-methylpyrrolidinium bis(trifluoromethyl sulfonyl)imide ([Py<sub>1,4</sub>][NTf<sub>2</sub>]), ethyltributylphosphonium bis(trifluoromethyl sulfonyl)imide ([P<sub>2,4,4,4</sub>][NTf<sub>2</sub>]), 1-butyl-1-methylpiperidinium bis(trifluoromethyl sulfonyl)imide ([PP<sub>1,4</sub>][NTf<sub>2</sub>]), tributylmethylammonium bis(trifluoromethyl sulfonyl)imide ([N<sub>1,4,4,4</sub>][NTf<sub>2</sub>]), 1-ethyl-3-methylimidazolium bis(trifluoromethylsulfonyl)imide ([C<sub>2</sub>mim][NTf<sub>2</sub>]), 1-ethyl-2, 3-dimethylimidazolium bis(trifluoromethylsulfonyl)imide [C<sub>2</sub>C<sub>1</sub>mim][NTf<sub>2</sub>], 1-butyl-3-methylimidazolium bis(trifluoromethylsulfonyl)imide ([C<sub>4</sub>mim][NTf<sub>2</sub>]), 1-decyl-3-methylimidazolium bis(trifluoromethylsulfonyl)imide ([C<sub>10</sub>mim][NTf<sub>2</sub>]), 1-butyl-3-methylimidazolium hexafluorophosphate ([C<sub>4</sub>mim][PF<sub>6</sub>]), 1-ethyl-3-methylimidazolium tetrafluoroborate ([C<sub>2</sub>mim][BF<sub>4</sub>]), 1-ethyl-3-methylimidazolium trifluoromethanesulfonate ([C<sub>2</sub>mim][TfO]), 1-ethyl-3-methylimidazolium trifluoroacetate ([C<sub>2</sub>mim][TFA]), 1-ethyl-3-methylimidazolium dicyanamide ([C<sub>2</sub>mim][DCA]), 1-ethyl-3-methylimidazolium thiocyanate ([C<sub>2</sub>mim][SCN]), 1-ethyl-3-methylimidazolium hydrogen sulfate ([C<sub>2</sub>mim][HSO<sub>4</sub>]), 3-ethyl-1-methyl-1H-imidazolium perchlorate

([C<sub>2</sub>mim][ClO<sub>4</sub>]), 1-ethyl-3-methylimidazolium acetate ([C<sub>2</sub>mim][ACO]), 1-butyl-3-methylimidazolium iodide ([C<sub>4</sub>mim][I]), 1-hexyl-3-methylimidazolium bromide ([C<sub>6</sub>mim][Br]), 1-hexyl-3-methylimidazolium nitrate ([C<sub>6</sub>mim][NO<sub>3</sub>]), were purchased from Lanzhou Yulu Fine Chemical Co., Ltd. (GanSu, China) and have a purity >99%. All other reagents were used as received without further purification.

**Synthesis of the PEA elastomers:** First, single-network films were prepared by free radical polymerization of a solution of EA monomer, EGDMA as cross-linker (0.34 ~ 2.72 mol% relative to monomer), and PBPO as white light photoinitiator (1.16 mol% relative to monomer). After the reactants were dissolved in toluene as solvent, the mixture was poured in a 0.3 mm-thick glass mold. The polymerizations were initiated by the white light and left to proceed for one hour. The samples were then extracted from the mold and immersed in toluene/cyclohexane mixtures to extract any unreacted species. The single-network films were finally dried under vacuum at 80 °C overnight and then stored at room temperature until later use.

Starting from the single-network film, PEA elastomer was prepared following swelling and polymerization sequence. Briefly, a piece of single-network film was swollen in a bath composed of EA as monomer, EGDMA as cross-linker (0.01 mol% of monomer), and PBPO as photoinitiator (0.01 mol% of monomer). Once swollen to equilibrium, the sample was carefully extracted from the monomer bath and placed between the poly(ethylene terephthalate) sheet and glass plate. Then, the whole sample's holder was exposed to the white light for one hour to initiate and complete the

polymerization. After being dried in a vacuum at 80 °C overnight, the PEA elastomer was stored at room temperature for later use.

**Synthesis of the representative ionic liquids, [C<sub>2</sub>mim][NTf<sub>2</sub>]:** A solution of 1-methyl imidazole and ethyl bromide in cyclohexane was heated at 80 °C under reflux for 24 h. After evaporation, the product, 1-ethyl-3-methyl imidazolium bromide ([C<sub>2</sub>mim]Br), was obtained by repeated recrystallization from ethyl acetate/isopropyl alcohol (V/V, 1/1). Then, the anion exchange reaction was carried out by heating an equimolar mixture of [C<sub>2</sub>mim]Br and Li[NTf<sub>2</sub>] in water at 70 °C for 24 h. The obtained [C<sub>2</sub>mim][NTf<sub>2</sub>] was repeatedly washed with pure water and then dehydrated under vacuum at 120 °C for 72 h.

**Preparation of the ionogels:** The ionogels with different IL contents were prepared by the following procedure. Small pieces of elastomer (m<sub>1</sub>) were immersed in IL/ethanol (*i.e.*, 1/5 or 1/8 V/V) mixture for 24 h. Then, the samples containing IL/ethanol mixture were removed from the ethanol solution and dried in a vacuum at 70 °C overnight. The weight of the prepared ionogel (m<sub>2</sub>) was measured. The IL content in each ionogel was calculated by the following equation

$$\text{IL content (wt\%)} = (m_2 - m_1) / m_2 \times 100\%$$

**Determination of fracture energy:** We used the pure shear test to measure the fracture energy. A notch of 10 mm length was made in the middle of specimen, whose total width was a<sub>0</sub> = 30 mm. The specimen was fixed in two clamps with a pre-set distance of L<sub>0</sub> = 5 mm. The thickness (b<sub>0</sub>) depends on the sample itself. The specimen was

subjected to uniaxial tension with a strain rate of 5 mm/min. The fracture energy ( $\Gamma$ ) was calculated from

$$\Gamma = U(L_c)/a_0b_0$$

where  $U(L_c)$  is the strain energy calculated by integration of the stress-strain curve of an un-notched specimen until  $L_c$  ( $L_c$  is the distance between the clamps when crack starts to propagate).

***Characterization and measurements:*** Differential scanning calorimetry (DSC) data were obtained using a TA Instrument (DSC Q2000) with a scan rate of 10 °C min<sup>-1</sup> under dry nitrogen environment. Thermal gravimetric analysis (TGA) measurements were performed on a TGA Q500 via scanning a temperature range from room temperature up to 600 °C (10 °C min<sup>-1</sup>) under dry nitrogen environment. Structure and morphology of the samples were characterized using scanning electron microscope (SEM, Hitachi 7500 at 15 kV) equipped with an energy dispersive X-ray (EDX) analyzer, environment scanning electron microscope (ESEM, Quanta FEG 250), and confocal laser scanning microscope (CLSM, FV1000-D). Infrared spectra were collected using an attenuated total reflectance Fourier transform infrared spectroscopy (ATR-FTIR) under atmospheric conditions. The transparency of the ionogel was characterized by using a UV-visible spectrophotometer (UV-3600 SHIMADZU Spectrometer) to scan wavelengths from 400 nm to 800 nm. Proton nuclear magnetic resonance (<sup>1</sup>H NMR) spectra were recorded using a Bruker AM 400 spectrometer with chloroform-*d* (CDCl<sub>3</sub>) as the solvent. Uniaxial tensile tests were performed using a universal tensile tester (Mark-10/ESM301) with a load cell of 10 N. The ionogel was

cut into a 15 mm long, dumbbell-shaped testing sample with a length of 4 mm at the narrowest position. The thickness depends on the sample itself. Nominal tensile stress was defined as the force divided by the original cross-sectional area. The tensile strain ( $\epsilon$ ) were determined as the elongation ( $\Delta L$ ) divided by the initial length ( $L_0$ ) ( $\epsilon = \Delta L/L_0 \times 100\%$ ). The Young's modulus of the ionogels was calculated by fitting the initial linear regime of stress-strain curve. The electromechanical behaviors of the ionogels were measured by using CHI660E electrochemical workstation.

## Supporting figures:

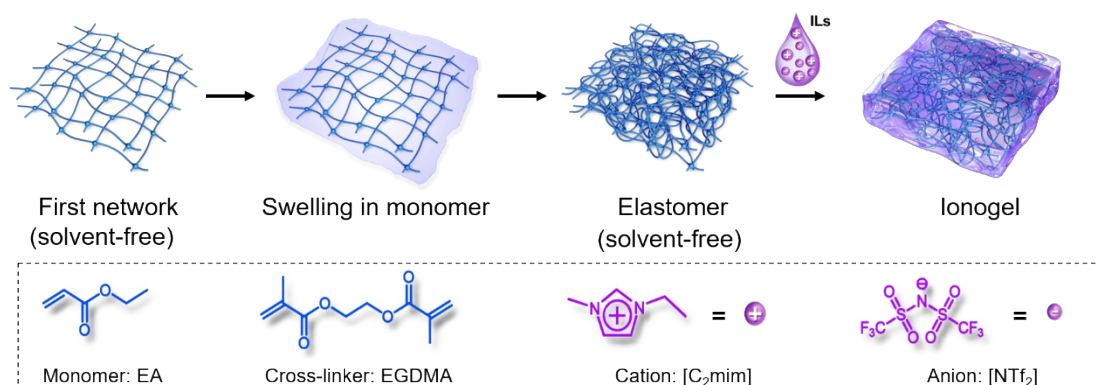


**Fig. S1** Schematic illustration of the fabrication process of the ionogel.

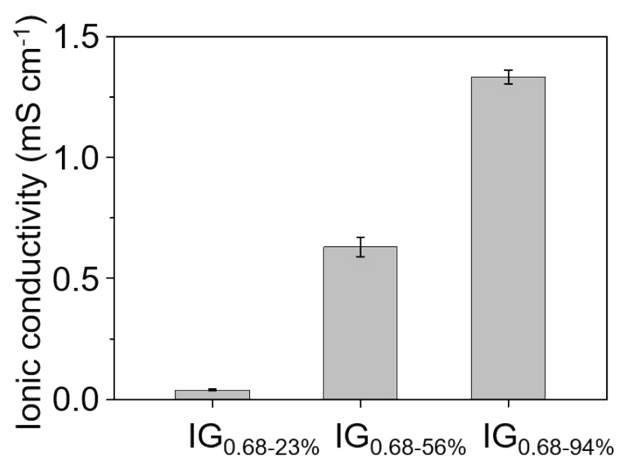


**Fig. S2** Ionic conductivity of the ionogels with different weight fractions of [C<sub>2</sub>mim][NTf<sub>2</sub>] at 20 °C. The ionic conductivity of the ionogel increased with the increase of IL content.

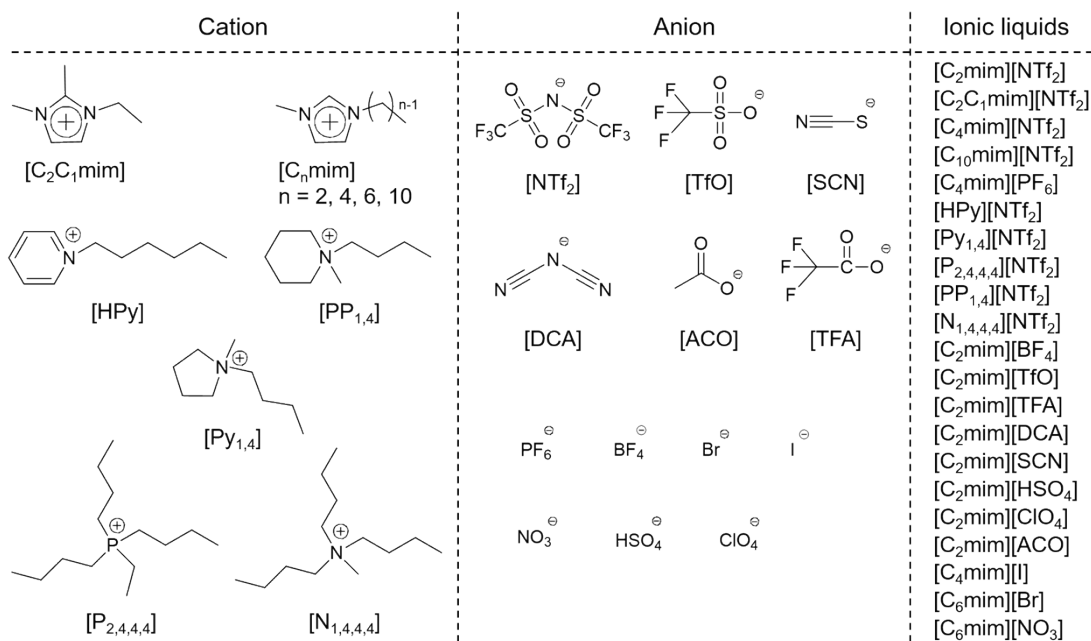


**Fig. S3** ILs used in this study and their chemical structures.

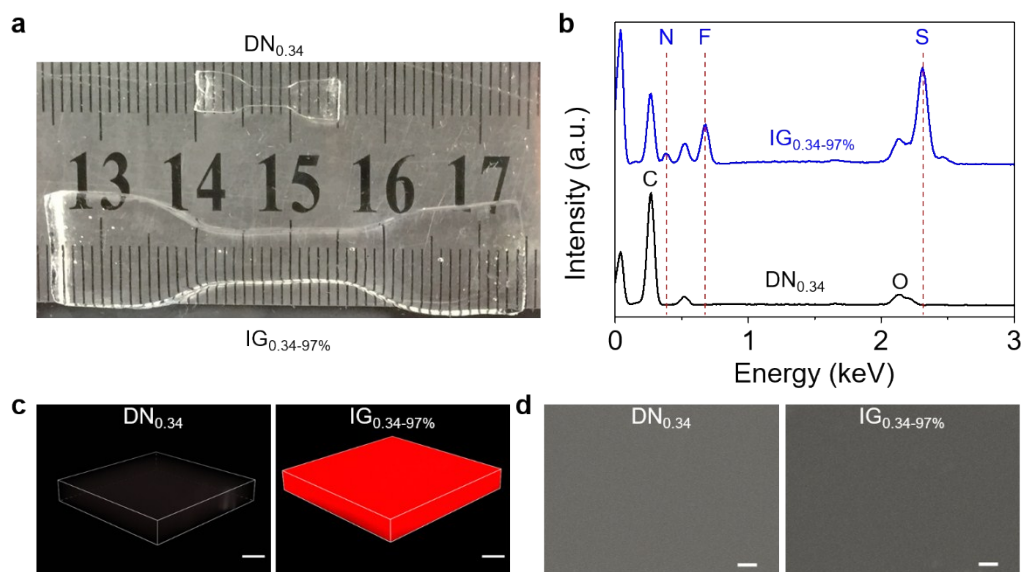


**Fig. S4** Compatibility between the elastomer and  $[\text{C}_2\text{mim}][\text{NTf}_2]$ . a) Photographs of the dumbbell-shaped  $\text{DN}_{0.34}$  and  $\text{IG}_{0.34-97\%}$ , respectively. b) EDX elemental analysis spectra of the cross-sectional  $\text{DN}_{0.34}$  and  $\text{IG}_{0.34-97\%}$ , respectively. c) CLSM observations of the cross-sectional  $\text{DN}_{0.34}$  and  $\text{IG}_{0.34-97\%}$ , respectively. Scale bar: 50  $\mu\text{m}$ . d) Cross-sectional SEM images of the  $\text{DN}_{0.34}$  and  $\text{IG}_{0.34-97\%}$ , respectively. Scale bar: 10  $\mu\text{m}$ .

**Discussion:** The  $\text{DN}_{0.34}$  was submerged in  $[\text{C}_2\text{mim}][\text{NTf}_2]$  at room temperature until equilibrium was established. IL content in the corresponding ionogel reached up to 97 wt%, which is substantially higher than those of most ionogels reported in the literature.<sup>19–31, 36, 37, 39–41</sup> The ionogel is highly transparent even at high IL weight fraction, suggesting the homogeneity of  $[\text{C}_2\text{mim}][\text{NTf}_2]$  in the elastomer (Fig. S4a). In comparison with the elastomer that only displays C and O element peaks, the ionogel appears three new peaks corresponding to N, F, and S elements, due to the presence of  $[\text{C}_2\text{mim}][\text{NTf}_2]$  (Fig. S4b). In order to CLSM observation, a piece of elastomer was immersed in a Rhodamine B/ethanol mixture for 24 h. The sample containing IL/ethanol mixture were removed from the ethanol solution and dried in a vacuum at 70 °C overnight. No fluorescence was observed, indicating that the elastomer could not be stained with Rhodamine B (Fig. S4c). By contrast, after a piece of elastomer was immersed in a Rhodamine B/ $[\text{C}_2\text{mim}][\text{NTf}_2]$  mixture for enough time, Rhodamine B was uniformly distributed in the prepared ionogel, further revealing the high

homogeneity of the iongels without any phase separation. The cross-sectional SEM images show that both the elastomer and iongel have a smooth and dense cross section without pores (Fig. S4d).

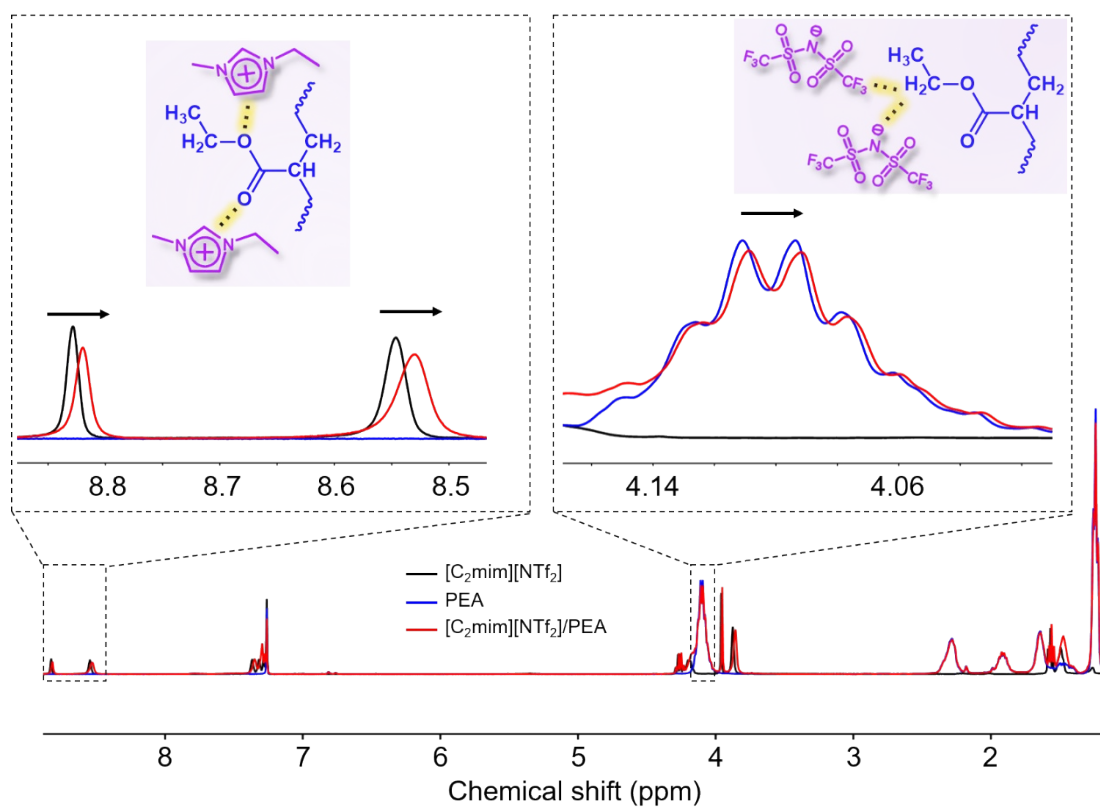


**Fig. S5**  $^1\text{H}$  NMR spectra of  $[\text{C}_2\text{mim}][\text{NTf}_2]$ , PEA, and  $[\text{C}_2\text{mim}][\text{NTf}_2]/\text{PEA}$ , respectively. Inset: Schematic hydrogen bonding between the  $[\text{C}_2\text{mim}][\text{NTf}_2]$  and PEA.

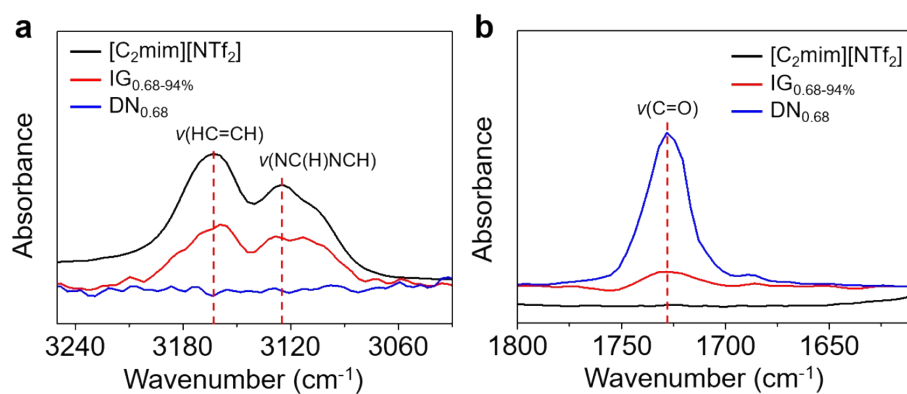


**Fig. S6** ATR-FTIR spectra of a) cation stretching region and b) carbonyl stretching region, respectively.

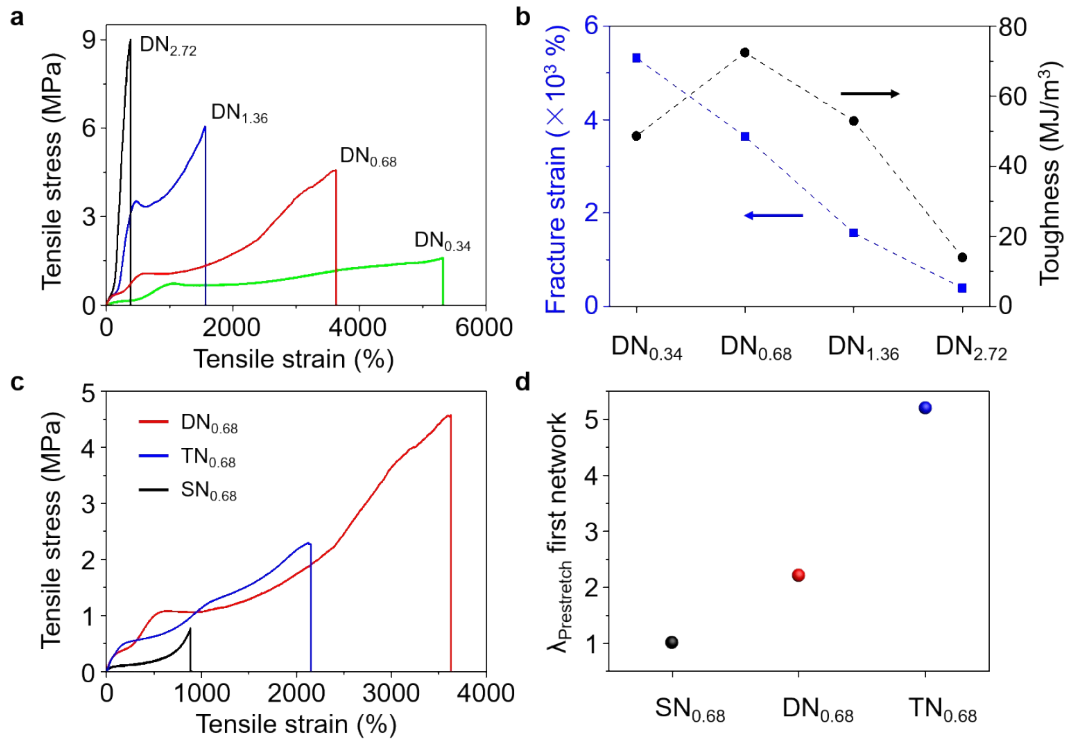


**Fig. S7** Stretching test of the polymer network. a) Tensile stress-strain curves of the elastomer with various cross-linker concentration in the first network. b) Fracture strain and toughness of the elastomers with various cross-linker concentration in the first network, respectively. The toughness was calculated from the area under the stress-strain curve of the tensile tests. c) Tensile stress-strain curves of the single-network elastomer (SN<sub>0.68</sub>), double-network elastomer (DN<sub>0.68</sub>), and triple-network elastomer (TN<sub>0.68</sub>), respectively. d) Prestretching of the first network. TN<sub>0.68</sub> was prepared following the same swelling/polymerization process but starting from the DN<sub>0.68</sub>. In order to determine the composition of the final DN<sub>0.68</sub> and TN<sub>0.68</sub>, we used the thickness of the samples. In brief, before swelling, the thickness ( $h_{\text{SN}}$ ) of the piece of single-network elastomer was first measured. Then, the same characteristics were collected from the final double/triple network sample ( $h$ ). The prestretch of chains of the first network ( $\lambda_{\text{Prestretch}}$ ) was determined using the thicknesses. The  $\lambda_{\text{Prestretch}}$  was calculated as  $h/h_{\text{SN}}$ .

**Discussion:** Given the fact that the mechanical integrity of the ionogels is due to the polymer network, the mechanical behavior of the PEA polymer network was analyzed

in detail. Because the decrease in cross-linker concentration gives a network with longer chains between cross-links and larger equilibrium swelling ratio, a lower concentration of cross-linker in the first network leads to higher stretchability and lower stiffness of the elastomer (Fig. S7a). To prepare a high-performance ionogel with a unique combination of relatively high stretchability, stiffness, extraordinary toughness, and good self-recoverability, the optimal composition of cross-linker in the first network was determined to be 0.68 mol% (Fig. S7b). More interestingly, the double-network elastomer shows stretchability and toughness higher than the corresponding single-network elastomer and derived triple-network elastomer (Fig. S7c). In the triple-network elastomer, the first and second network chains were highly stretched owing to swelling (Fig. S7d). The high level of prestretching of first and second network chains led to lower stretchability of the triple-network elastomer.

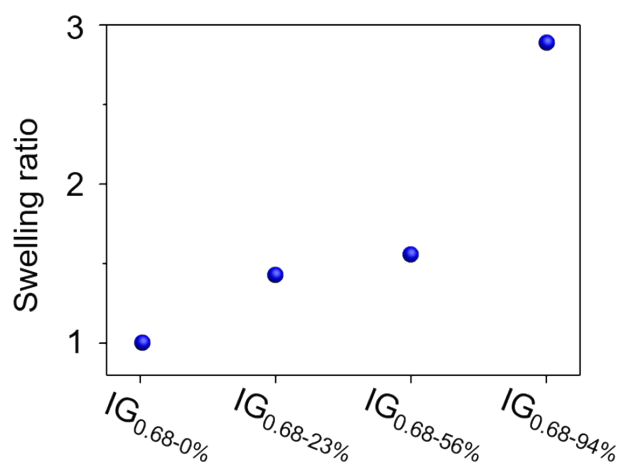


**Fig. S8** Swelling ratio of ionogels (IG<sub>0.68-y</sub>). We used the thickness of the samples to determine the swelling ratio. Briefly, before swelling, the thickness ( $h_{DN}$ ) of elastomer was first measured. Then, the same characteristics were collected from the resulting ionogels ( $h_{IG}$ ). The swelling ratio was calculated as  $h_{IG}/h_{DN}$ .

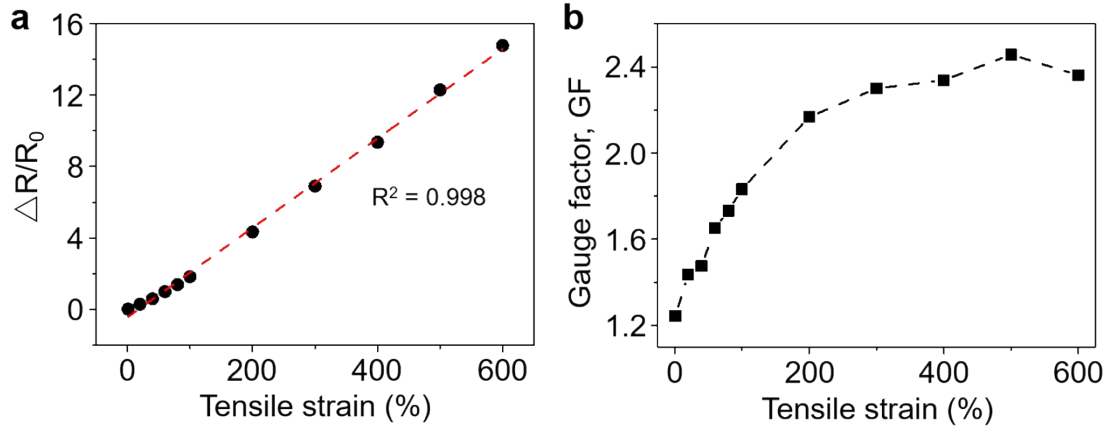


**Fig. S9** a) Relative resistance change of the ionogel-based sensor as a function of tensile strain. b) Gauge factor (GF) versus tensile strain for the ionogel-based sensor.

**Discussion:** Relative resistance change [ $\Delta R/R_0 = (R - R_0)/R_0$ , where  $R_0$  is the initial resistance,  $R$  is the resistance in the stretched state] of the ionogel-based sensor increased with increasing tensile strain (Fig. S9a). Significantly, the relation between the relative resistance change and tensile strain (from 0% to 600%) has an exceptional linearity  $R^2$  value of 0.998, which is the highest value among all of the reported strain sensors with at least 100% stretchability.<sup>36</sup> Gauge factor (GF, defined as  $GF = (\Delta R/R_0)/\epsilon$ , where  $\epsilon$  is the applied tensile strain) of the ionogel-based sensor increased as the tensile strain increased (Fig. S9b). For example, the GF was 1.24 at 1% strain and increased to 1.83 at 100% strain, which is higher than that of other ionogel-based strain sensor ( $\sim 0.95$  at 55% strain).<sup>36</sup>

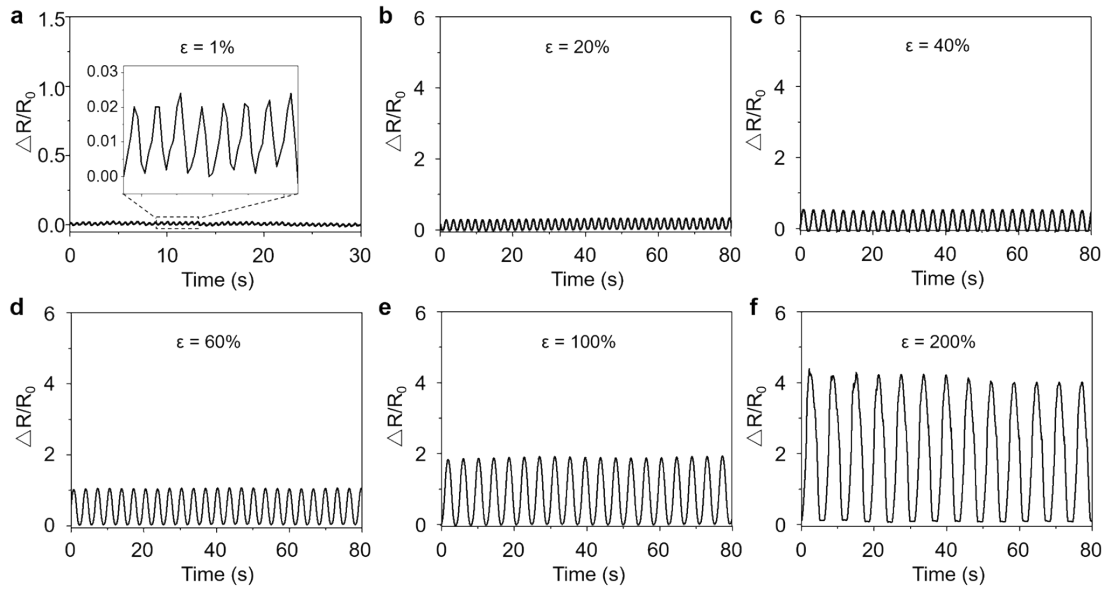


**Fig. S10** Electromechanical properties of the ionogel-based sensor. a–f) Relative changes in resistance versus time for the sensor during loading–unloading cycles under 1, 20, 40, 60, 100, and 200 % strain, respectively.

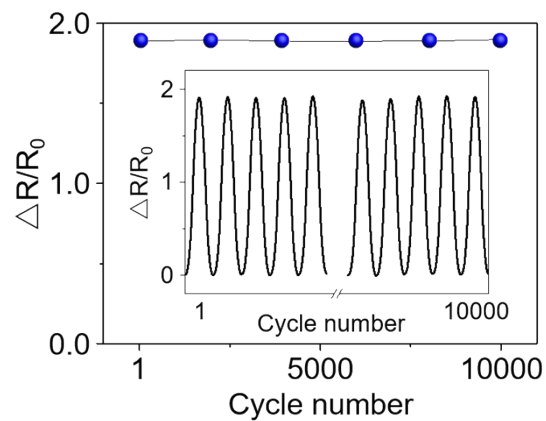


**Fig. S11** The long-term stability of the ionogel-based sensor by repeatedly applying a maximum tensile strain of 100% for 10000 cycles.

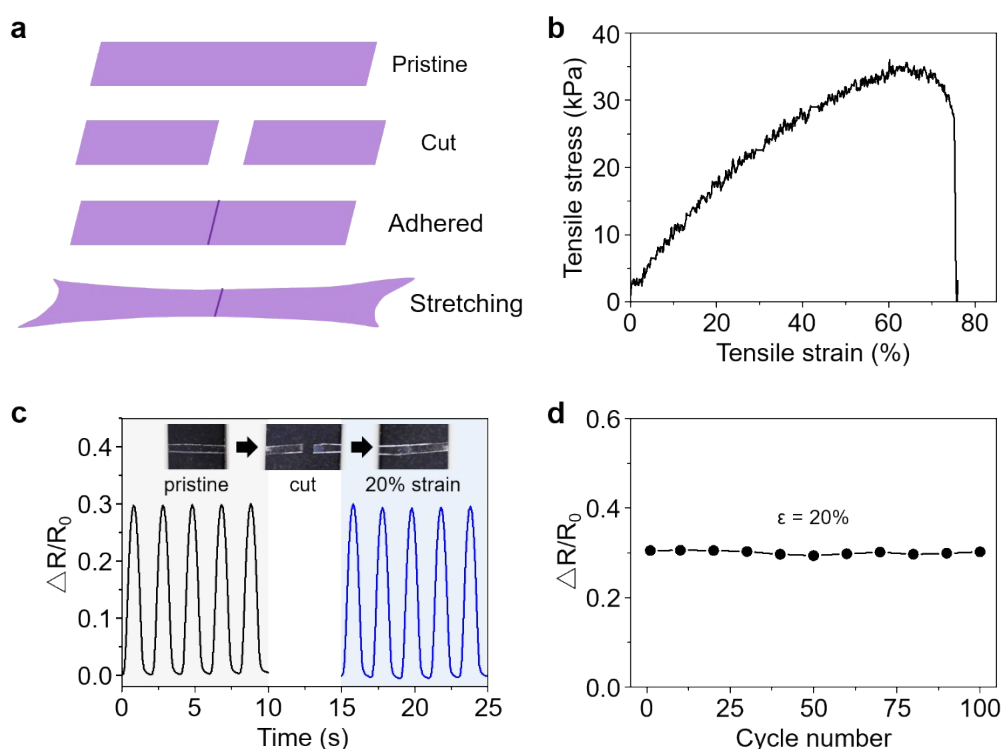


**Fig. S12** Adhesive and electrical properties of the ionogel. a) Schematic illustration of the strong adhesive property of the ionogel: the pristine ionogel was cut into two pieces, and then the two resulting surfaces were brought together at room temperature, junction between the two cut ionogels formed immediately. Importantly, the joined ionogel retain its integrity even at stretch. b) Tensile stress–strain curve of the joined ionogel, showing that the sample can be stretched to over 70%. c) Relative changes in resistance versus time for the pristine ionogel and joined ionogel under a maximum tensile strain of 20%, respectively. d) The change of relative resistance of the joined ionogel by repeatedly applying a maximum tensile strain of 20% for 100 cycles.

**Discussion:** Given the strong self-adhesion property of the ionogels, after a pristine ionogel was cut into two pieces, the joined ionogel after adhering at room temperature retained its integrity even at stretch (Fig. S12a). The joined ionogel could be stretched to over 70% (Fig. S12b). The dynamic response for both the pristine and joined ionogel under a maximum tensile strain of 20% is near-identical (Fig. S12c). Even after 100

cycles of stretching-releasing, the resistance variation of the joined ionogel remained nearly unchanged (Fig. S12d), revealing its excellent robustness and cycling stability. This characteristic, similar to the self-repairable function, promises the sensor to greatly improve long-term reliability upon mechanical loading.

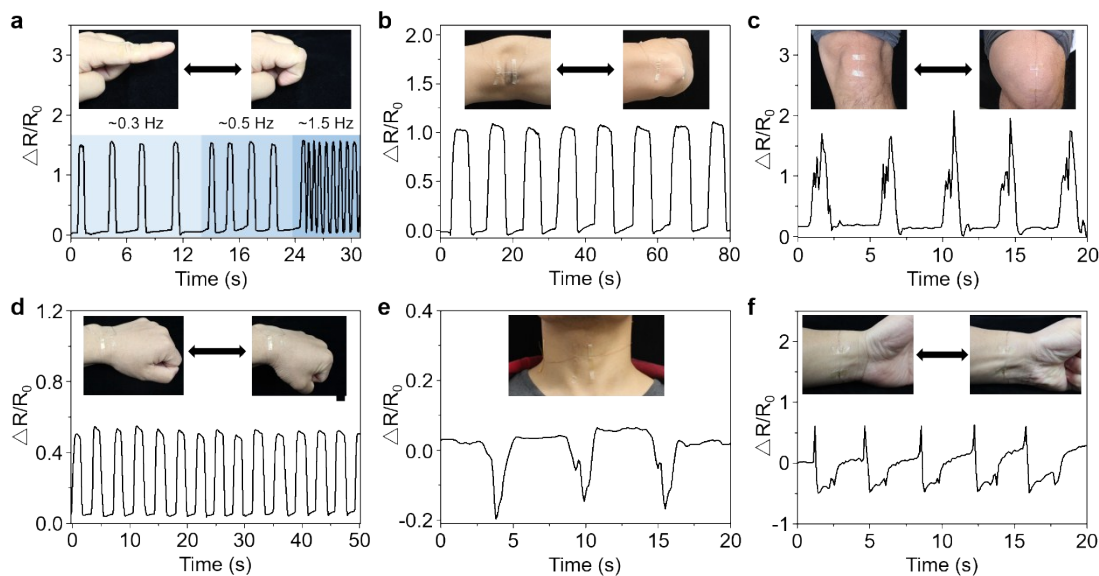


**Fig. S13** Human motion detection by the ionogel-based sensor. Monitoring of various human motions in real time through the physical movements of various body parts: a) index finger bending-releasing motions with different frequencies, b) elbow joint bending-releasing motions, c) knee joint bending-releasing motions, d) wrist bending-releasing motions, e) swallowing, f) muscular tension and relaxation.

**Discussion:** To demonstrate the potential of the ionogel-based sensor in emerging wearable electronics, we attached the sensor on the skin to detect the bending and stretching of the human body. For example, when attached on the finger, the finger bending-releasing motions can be easily reflected by the change in the relative resistance of the sensor. The relative resistance increased rapidly upon the bending of the index finger, recovering its original value once the finger was full released. The finger-mounted sensor exhibited reliable and rapid dynamic responses to various frequencies (0.3, 0.5, and 1.5 Hz). By attaching the ionogel onto the elbow and knee joint, the joint bending motions were also detected in real time and in situ. Compared with above joint bending motions, the maximum change in the relative resistance during

wrist bending-releasing motions is smaller, resulting from the smaller strain. Moreover, when fixed to the throat, swallowing could be monitored by detecting movement of the laryngeal prominence. The sensor could also be used to detect tiny motions of muscles during its tension and relaxation processes.

## 2. Supplementary Tables

**Table S1.** Formulation of DN<sub>x</sub> prepared from first networks prepared in toluene.

Sample <sup>a)</sup>	[EGDMA] (mol %) <sup>b)</sup>	EA (mL)	Toluene (mL)	[PBPO] (mol %) <sup>c)</sup>
DN <sub>2.72</sub>	2.72	1.17	1.17	1.16
DN <sub>1.36</sub>	1.36	1.17	1.17	1.16
DN <sub>0.68</sub>	0.68	1.17	1.17	1.16
DN <sub>0.34</sub>	0.34	1.17	1.17	1.16

a) DN<sub>x</sub>, where ‘x’ is the cross-linker concentration of the first network. The cross-link density of the second network was fixed to 0.01 mol%; b) [EGDMA] = 100 × n<sub>EGDMA</sub>/n<sub>EA</sub>, with n<sub>EA</sub> and n<sub>EGDMA</sub> the number of moles of EA and EGDMA, respectively; c) [PBPO] = 100 × n<sub>PBPO</sub>/n<sub>EA</sub>, with n<sub>EA</sub> and n<sub>PBPO</sub> the number of moles of EA and PBPO, respectively.

**Table S2.** Position and assignment of the important IR signals.

Materials	$\nu(\text{HC}=\text{CH})$	$\nu(\text{NC}(\text{H})\text{NCH})$	$\nu(\text{C}-\text{H})$	$\nu(\text{C}=\text{O})$	$\nu(\text{SO}_2)$	$\nu(\text{CF}_3)$	$\nu(\text{SNS})$
DN <sub>0.68</sub>	no	no	2981	1728	no	no	no
[C <sub>2</sub> mim][NTf <sub>2</sub> ]	3162	3125	no	no	1354, 1334, 1139	1227, 1195	1058
IG <sub>0.68-94%</sub>	3162	3125	3000	1728	1347, 1330, 1134	1225, 1176	1052

### 3. Supplementary Video

*Video S1.* Demonstration of the adhesive property of the ionogel. The tough junctions formed instantly by attaching the ionogel to ionogel itself and metals including copper (Cu) and aluminum (Al) without any modification. The three junctions can endure large stretch ratios ( $\lambda = 2.9$ ), demonstrating that the adhesions between ionogel and ionogel as well as metals are quite strong.